GATE SIMULATION STUDY OF THE 24-MODULE J-PET SCANNER: DATA ANALYSIS AND IMAGE RECONSTRUCTION*

M. Dadgar[a], P. Kowalski[b]

for the J-PET Collaboration

[a]Faculty of Physics, Astronomy and Applied Computer Science
Jagiellonian University, 30-348 Kraków, Poland
[b]Department of Complex Systems, National Centre for Nuclear Research
05-400 Otwock-Świerk, Poland

(Received December 9, 2019)

The Jagiellonian Positron Emission Tomograph (J-PET) is a novel PET device that, in contrast to commercial PET scanners, is based on plastic scintillator strips. Modular J-PET is the latest prototype that consists of 24 modules arranged in a cylinder. In this study, 6 point-like sources defined in the NEMA spatial resolution standard were simulated twice with total activities of 60 kBq and 60 MBq, respectively. Results of simulations were processed with the GOJA software and reconstructed with the QETIR package.

DOI:10.5506/APhysPolB.51.309

1. Introduction

Nowadays, Positron Emission Tomography (PET) is widely used in many clinical, cancer and even metabolism research centers all around the world [1]. Many research teams try to improve performance of PET scanners. New detectors are developed to achieve this goal [2–5]. Sensitivity of the PET scanner is one of performance characteristics that shows its quality [2, 6]. It is expressed as the true coincidence events rate normalized to the total activity of the source. Nowadays, most of clinical PET scanners have almost 20 cm axial field of view only [7]. If the axial field of view was extended, also the sensitivity could be improved. However, costs of extension, by additional crystal rings, increases proportionally to the axial field of view.

* Presented at the 3rd Jagiellonian Symposium on Fundamental and Applied Subatomic Physics, Kraków, Poland, June 23–28, 2019.

The Jagiellonian Positron Emission Tomograph (J-PET) is a novel PET scanner constructed from plastic scintillators [8–12]. It may be used not only for PET imaging but also for studies of positronium state [4] or quantum entanglement [13]. The main geometrical difference between the J-PET tomograph and other PET scanners is an arrangement of scintillators and photodetectors [8]. In traditional PET, a photodetector is located behind the scintillator in the radial direction. When enlarging traditional PET devices, the number of needed additional scintillators and photodetectors is proportional to the length of the extension. In the J-PET, to enlarge the axial field of view, only the length of the scintillator strips must be increased. 24-module J-PET is the latest prototype of the J-PET Collaboration equipped with Silicon Photomultiplier Matrices (SiPMs). Its geometry is described in the next section.

Geant4 Application for Tomography Emission (GATE) is an essential tool in simulations of PET prototypes that allows researchers to design and study new geometries of the tomograph, to optimize its performance or to simulate data for image reconstruction [14]. The aim of the study described in this article was to perform simulations for image reconstruction and to reconstruct obtained data for the 24-module J-PET prototype. To reconstruct images, the Quantitative Emission Tomography Iterative Reconstruction (QETIR) software was adapted [15].

2. Geometry and simulation parameters

The J-PET prototype consists of 24 detection units called modules. Every module is made of 13 strips of EJ-230 plastic scintillators [16] with dimension of $6 \times 25 \times 500$ mm^3. Each next scintillator in a module is placed parallelly to the previous one (parallel sides have dimension of 25×500 mm^2). All scintillator strips are equipped with SiPMs attached to both ends, as shown in Fig. 1 (left). The modules are arranged in a cylindrical structure to create modular J-PET (Fig. 1 (right)).

In this study, 24-module J-PET prototype was simulated with 6 point-like sources according to the NEMA-NU-2-2019 standard [17]. These sources were placed in the following positions (the center of the coordinate system is the center of the field of view): source N_1 — (1, 0, 0) cm, N_2 — (1, 0, 18.75) cm, N_3 — (10, 0, 18.75) cm, N_4 — (10, 0, 0) cm, N_5 — (20, 0, 0) cm and N_6 — (20, 0, 18.75) cm. The simulation was executed for two different activities of sources to study an influence of activity on output data. Total activities in these two simulations were 60 kBq and 60 MBq, respectively.

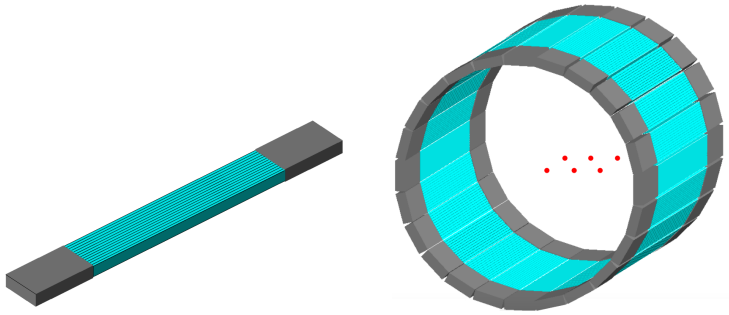

Fig. 1. (Color online) Left: GATE visualization of a single module with 13 strips of plastic scintillators (light gray/cyan) and SiPMs and readout electronics at their ends (gray). Right: 24-module J-PET with 6 point-like sources (black/red); the sources are enlarged to be visible in GATE visualization.

3. Data analysis

Results of the GATE simulations were saved as ROOT files that include all the information about detected events. To analyze these raw ROOT outputs GATE Output J-PET Analyzer (GOJA) was used. It is a software developed by the J-PET Collaboration [2]. Alongside many capabilities that GOJA has, it can pre-select events and produce a listmode format (LMF) file, which may be used for the image reconstruction. GOJA's LMF include information about positions and times of interactions in a coincidence, type of coincidence and information about annihilation point.

A coincidence is defined as an event in which in a fixed time window of 3 ns, there are exactly 2 interactions with energy deposited higher than 200 keV and any number of interactions with energy deposited smaller than this fixed threshold. All coincidences detected in the GATE simulation are categorized in 4 different types: true, phantom-scattered, detector-scattered and random. True coincidences refer to detection of 2 photons emitted from a single e^+e^- annihilation, under the condition that none of them was scattered before detection. In phantom-scattered coincidences, at least one of detected photons was scattered also in a phantom[1] before the detection. (In this study, there is no phantom so there are no phantom-scattered coincidences.) Detector-scattered coincidences refer to the events in which at least one of photons was scattered in the detector before a final detection. Random coincidences are the events in which photons originate from two different annihilations [18]. True coincidences contribute in image reconstruction positively, while scattered and random coincidences decrease the image quality [19].

[1] The phantom is a volume imitating the patient's body, *e.g.* it may be a polyethylene cylinder [6].

4. Image reconstruction

Data obtained from the GATE simulations and pre-processed with the GOJA software were further reconstructed with the QETIR software. QETIR is an image reconstruction software developed in the Medisip Ghent University Hospital. It reconstructs an image using both Time-Of-Flight (TOF) and non-TOF LMF data [15, 20]. Beside its image reconstruction application, QETIR allows one to generate sensitivity map for scanner sensitivity correction. In order to reconstruct an image with a QETIR LMF file, configuration files and the sensitivity map should be provided.

The LMF needed by QETIR for image reconstruction is a binary file that consists of 6 columns for non-TOF reconstruction or 7 columns for TOF image reconstruction. In both of these LMFs, first 6 columns are X_1, Y_1, X_1, X_2, Y_2, Z_2, which are positions of hits in mm. In a TOF LMF file, the 7^{th} column is time difference of these two hits in ps. To run QETIR, also 2 different configuration files must be prepared. First one contains the description of the scanner geometry in a way understandable by QETIR, second one contains information about reconstruction parameters, input files, voxel size, number of iterations *etc.* To obtain high image quality, also the sensitivity map of the J-PET scanner must be calculated and provided for the reconstruction step [21]. In Fig. 2, a transverse slice of the sensitivity map of the 24-module J-PET prototype is presented.

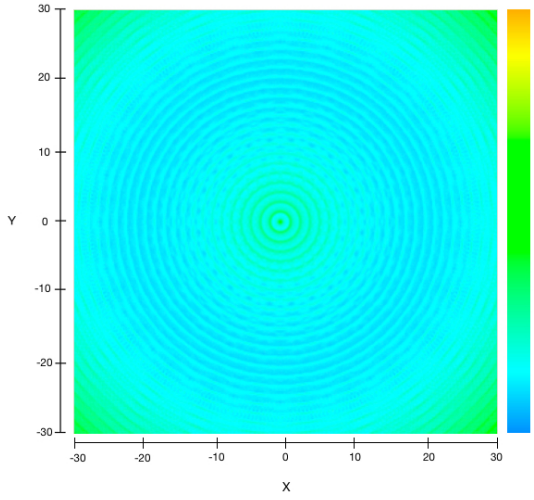

Fig. 2. Transverse view of the 24-module J-PET sensitivity map generated by QETIR with 2 mm slice thickness in center of field of view.

5. Results

In this study, the 24-module J-PET scanner with spatial resolution sources defined in NEMA-NU-2-2019 were simulated, firstly, with low activity of 60 kBq and secondly, with higher activity of 60 MBq. Analysis of results of GATE simulations shows that among all the possible coincidences, for an activity of 60 kBq, there are mainly true and detector-scattered coincidences, while the amount of random coincidences is negligible. The major percentage of coincidences for this low activity belongs to true events. For simulation with activity of 60 MBq alongside true coincidences and detector-scattered ones, there are many random coincidences (39% of all coincidences). The percentage of each type of coincidences for both activities are summarized in Table I.

TABLE I

The percentage of each type of coincidences for the two activities used.

Total activity of 6 point-like sources	True coincidences	Detector-scattered coincidences	Random coincidences
60 kBq	90%	10%	0%
60 MBq	55%	6%	39%

Figure 3 contains two scatter plots of angle differences *vs.* time differences for two activities used. The most obvious difference between plots is the background of plots which is due to the random coincidences.

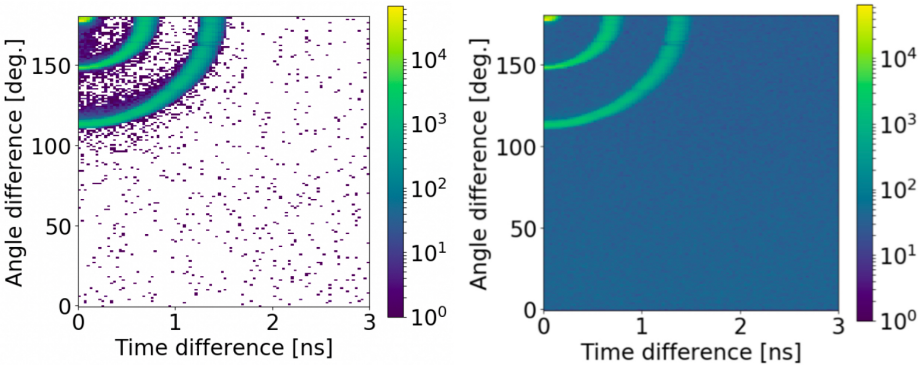

Fig. 3. Scatter plots of angle differences *vs.* time differences. Left: 60 kBq. Right: 60 MBq. The reason of difference between the plots is a presence of 39% random coincidences as a background in the right plot.

The final image of 6 point-like sources reconstructed in QETIR is shown in Fig. 4. To reconstruct this image, the LMF containing 1.6×10^6 coincidences was used. The sensitivity map applied to reconstruct images was generated in QETIR. The voxel size in this map was $2 \times 2 \times 2$ mm^3 and the image was reconstructed with the Maximum Likelihood Estimation Method (MLEM) algorithm [22].

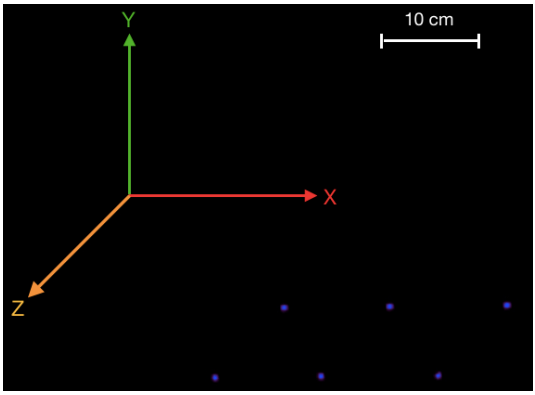

Fig. 4. QETIR MLEM reconstructed image of simulation data of 6 point-like sources distributed according to the NEMA-NU-2-2019 standards.

The amount of random coincidences grows with the total activity of the source. Both detector-scattered and random coincidences decrease quality of final reconstructed images. The influence of these false coincidences on the final image quality will be further investigated using reconstructions of more complex sources.

This work was supported by the Polish National Centre for Research and Development through grant INNOTECH-K1/IN1/64/159174/NCBR/12, the Foundation for Polish Science through the MPD and TEAM POIR.04.04. 00-00-4204/17, the National Science Centre, Poland (NCN) through grant No. 2016/21/B/ST2/01222.

REFERENCES

[1] Y.F. Tai, P. Piccini, *J. Neurol. Neurosurg. Psychiatry* **75**, 669 (2004).
[2] P. Kowalski *et al.*, *Phys. Med. Biol.* **63**, 165008 (2018).
[3] S. Cherry *et al.*, *J. Nucl. Med.* **59**, 3 (2018).
[4] P. Moskal, B. Jasińska, E.Ł. Stępień, S.D. Bass, *Nature. Rev. Phys.* **1**, 527 (2019).

[5] L. Raczyński *et al.*, *Nucl. Instrum. Methods Phys. Res. A* **764**, 186 (2014).
[6] *Performance Measurements of Positron Emission Tomographs, NEMA Standards Publication*, NEMA NU 2-2019.
[7] S. Niedźwiecki *et al.*, *Acta Phys. Pol. B* **48**, 1567 (2017).
[8] P. Moskal *et al.*, *Phys. Med. Biol.* **64**, 055017 (2019).
[9] G. Korcyl *et al.*, *IEEE Trans. Med. Imag.* **37**, 2526 (2018).
[10] L. Raczyński *et al.*, *Phys. Med. Biol.* **62**, 5076 (2017).
[11] M. Pałka *et al.*, *JINST* **12**, 08001 (2017).
[12] L. Raczyński *et al.*, *Nucl. Instrum. Methods Phys. Res. A* **786**, 105 (2015).
[13] P. Moskal *et al.*, *Eur. Phys. J. C* **78**, 970 (2018).
[14] S. Jan *et al.*, *Phys. Med. Biol.* **49**, 4543 (2004).
[15] H. Theon *et al.*, *Phys. Med. Biol.* **58**, 6459 (2013).
[16] D. Kamińska *et al.*, *Eur. Phys. J.* **76**, (2016).
[17] M. Pawlik-Niedźwiecka *et al.*, *Acta Phys. Pol. A* **132**, 1645 (2017).
[18] J.F. Oliver, M. Rafecas, *PLoS ONE* **11**, e0162096 (2016).
[19] P. Kowalski *et al.*, *Acta Phys. Pol. B* **47**, 549 (2016).
[20] S. Vandenberghe, Website of the MEDISIP group from the Ghent University Hospital, `http://medisip.ugent.be/?page_id=50#QETIR`
[21] P. Kowalski *et al.*, *Bio-Algorith. Med-Syst.* **10**, 85 (2014).
[22] A. Słomski *et al.*, *Bio-Algorith. Med-Syst.* **10**, 1 (2014).